First geoneutrino measurement in JUNO

Qishan Liu 刘琪汕
(on behalf of the JUNO Collaboration)
Institute of High Energy Physics

The JUNO Detector

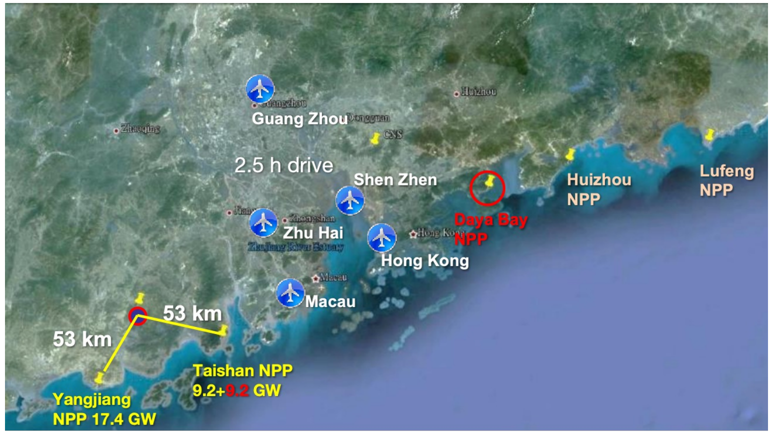

VETO System

- Top Tracker — plastic scintillator
- Water Pool: Ø43.5 m, H 44 m
- Earth magnetic-field shielding coils

Central Detector

- Stainless-steel structure · 35.4 m Ø acrylic sphere
- **20 kton** LAB-based liquid scintillator
- 17,612 × 20″ PMT + 25,600 × 3″ PMT
- ⇒ 78% photocathode coverage · 3%/√E resolution

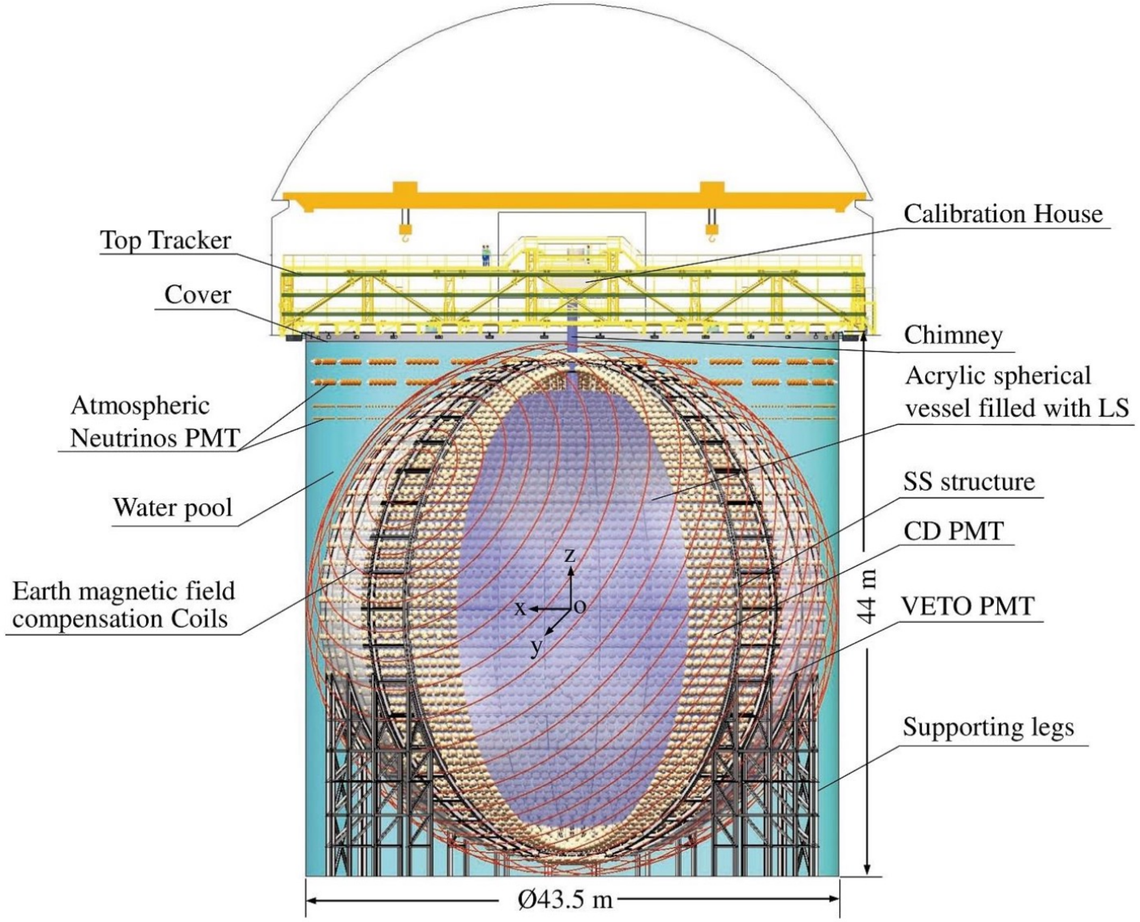

JUNO Detector Comparison

JUNO leads in target mass, light collection, energy resolution — and already the largest geo ν sample

Experiments	KamLAND	Borexino	SNO+	JUNO
Target Mass [tons]	1,000	300	780	**20,000**
Number of PMTs	~1,900	~2,200	~10,000	**17,612 + 25,600**
PMT Coverage	~34%	~30%	~50%	**78%**
Light Collection [p.e./MeV]	~250	~450	~520	**> 1,600**
Energy Resolution	$6\%/\sqrt{E}$	$5\%/\sqrt{E}$	$5\%/\sqrt{E}$	$3\%/\sqrt{E}$
Geo ν Events	183	53	35	**440**
Geo ν Measurement Time	5227 live days (2002–2020)	3263 live days (2007–2019)	685 live days (2022–2025)	**207 live days (2025–2026)**

JUNO's **20 kton target** + $3\%/\sqrt{E}$ energy resolution make it the world's most sensitive geoneutrino detector.

Geoneutrino Production & Spectra

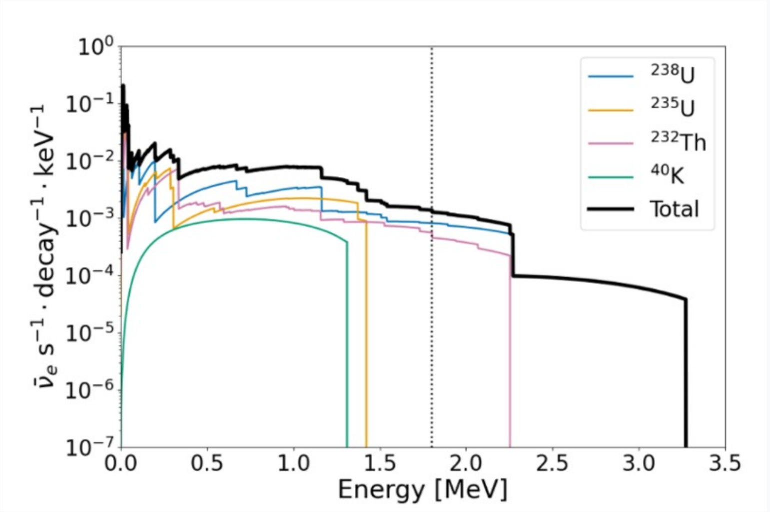

Geoneutrino energy spectra from ^{238}U, ^{235}U, ^{232}Th chains and ^{40}K. Vertical line: IBD threshold.

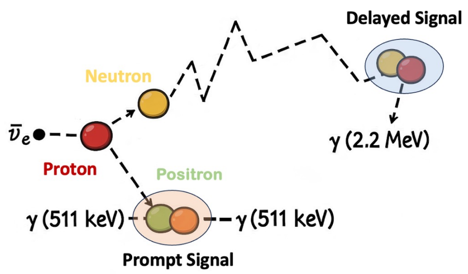

IBD reaction: prompt positron + delayed neutron capture

$$^{238}\mathrm{U} \to {}^{206}\mathrm{Pb} + 8\alpha + 6e^- + 6\bar{\nu}_e,\ \mathrm{Q} = 51.7\,\mathrm{MeV}$$
$$^{235}\mathrm{U} \to {}^{207}\mathrm{Pb} + 7\alpha + 4e^- + 4\bar{\nu}_e,\ \mathrm{Q} = 46.4\,\mathrm{MeV}$$
$$^{232}\mathrm{Th} \to {}^{208}\mathrm{Pb} + 6\alpha + 4e^- + 4\bar{\nu}_e,\ \mathrm{Q} = 42.6\,\mathrm{MeV}$$
$$^{40}\mathrm{K} \to {}^{40}\mathrm{Ca} + e^- + \bar{\nu}_e,\ \mathrm{Q} = 1.31\,\mathrm{MeV}\ (89.3\%)$$
$$^{40}\mathrm{K} + e^- \to {}^{40}\mathrm{Ar} + \nu_e,\ \mathrm{Q} = 1.504\,\mathrm{MeV}\ (10.7\%)$$

- Geoneutrinos from β-decays of **^{238}U, ^{235}U, ^{232}Th, ^{40}K** inside the Earth
- **Radiogenic heat** is in a well-known ratio to the number of emitted geoneutrinos
- IBD threshold ⇒ only **^{238}U & ^{232}Th** detectable; ^{40}K below threshold
- Distinct spectral shapes enable **U/Th separation**

Geoneutrino

A direct probe of Earth's interior composition

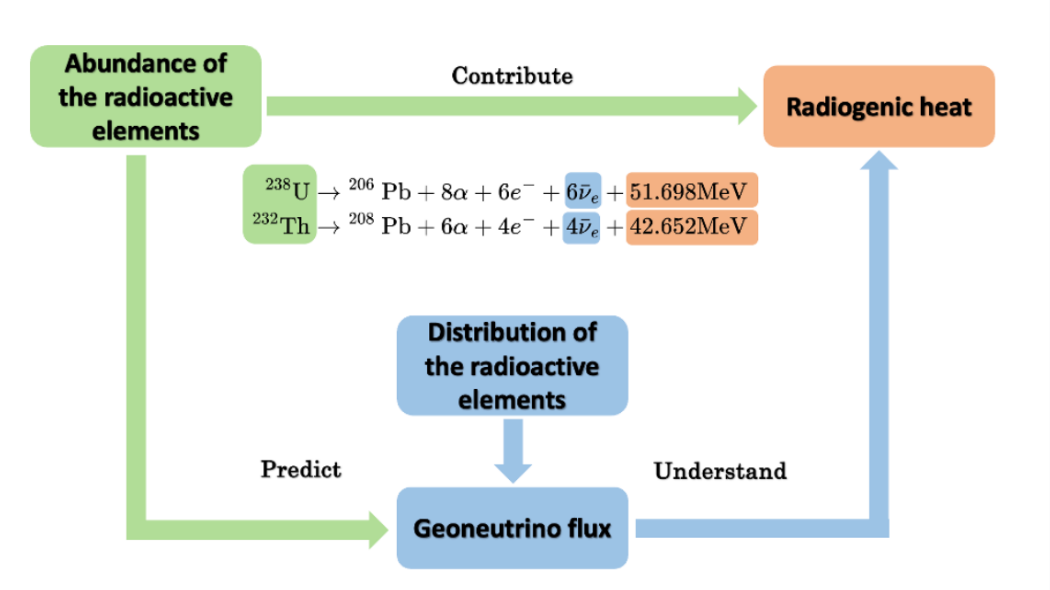

Geoneutrinos from U, Th, K decays throughout the Earth's crust and mantle

- Geoneutrino flux is **directly proportional** to the abundances of U and Th
- Their decays generate a **major fraction of Earth's radiogenic heat**
- **Direct constraints** on the terrestrial energy budget & interior structure

Geoneutrino Signal Component

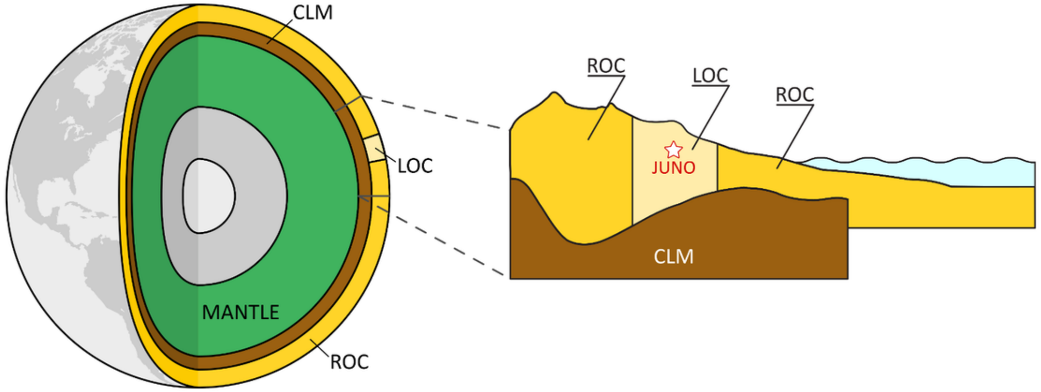

Earth's structure highlighting the components contributing to the geoneutrino signal.

- The **lithosphere** consists of the Earth's **crust** — split into the **Local Crust (LOC)** within a few hundred km of the detector and the **Rest of the Crust (ROC)** — plus the underlying **Continental Lithospheric Mantle (CLM)**.
- The experimental signal is the sum of two components: **mantle (M)** and **lithosphere (LS)**.
- The detector **cannot distinguish the neutrino direction**.
- To isolate the mantle contribution, the **lithosphere signal must be fixed and subtracted**.

Geoneutrino Signal Rate

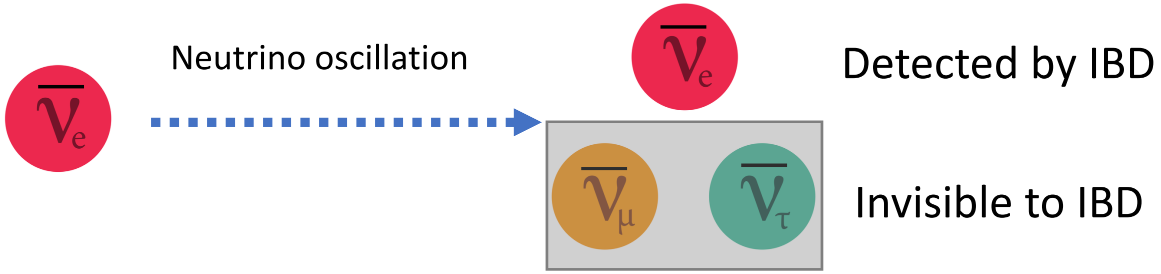

Abundances and density (g/cm³) from geo models

Neutrino oscillation probability

Distance factor (g/cm²)

$$f\left(i, E_{\bar{\nu}}\right) = \int P_{ee}\left(\left|\vec{r}-\vec{r}'\right|, E_{\bar{\nu}}\right) \cdot d^3r' \cdot \frac{a\left(i, \vec{r}'\right) \cdot \rho\left(\vec{r}'\right)}{4\pi\left|\vec{r}-\vec{r}'\right|^2}$$

Neutrino Flux (neutrino/s/cm²)

$$\Phi_{osc}(i, \vec{r}) = \epsilon_{i,\bar{\nu}} \cdot \int dE_{\bar{\nu}} \cdot \mathrm{Sp}\left(i, E_{\bar{\nu}}\right) \cdot f\left(i, E_{\bar{\nu}}\right)$$

Neutrino production rate (Neutrino/s/g)

Neutrino spectrum (/MeV)

Neutrino Signal

$$R[\mathrm{TNU}] = 10^{32} \cdot \frac{\text{seconds}}{\text{year}} \cdot \epsilon_{i,\bar{\nu}} \cdot \int dE_{\bar{\nu}} \cdot Sp\left(i, E_{\bar{\nu}}\right) \cdot \sigma_{\mathrm{IBD}}\left(i, E_{\bar{\nu}}\right) \cdot f\left(i, E_{\bar{\nu}}\right)$$

IBD events per 10^{32} free protons per year

IBD cross section (cm²)

Lithospheric and Mantle Models

Predicted geoneutrino signal contributions at JUNO

Lithospheric Models

Model	LOC Area (L×Lat)	S(U+Th) [TNU]
RRM	$6^\circ \times 4^\circ$	$30.9^{+6.5}_{-5.2}$
GIGJ	$6^\circ \times 4^\circ$	$28.9^{+5.5}_{-4.4}$
W20 [Crust 2.0]	$6^\circ \times 4^\circ$	$32.0^{+8.2}_{-6.6}$
W20 [Crust 1.0]	$6^\circ \times 4^\circ$	$31.7^{+8.4}_{-6.6}$
W20 [Litho 1.0]	$6^\circ \times 4^\circ$	$30.7^{+8.1}_{-6.4}$
JULOC	$10^\circ \times 10^\circ$	$40.4^{+5.6}_{-5.0}$
JULOC-I	$10^\circ \times 10^\circ$	$41.2^{+4.6}_{-3.3}$

TNU = Terrestrial Neutrino Unit — 1 IBD event per 10^{32} target protons per year with 100% efficiency.

Mantle Models (BSE classes)

BSE Class	$S_{\rm M}$(U+Th) [TNU]
Poor-H	$2.8^{+2.4}_{-1.9}$
Medium-H	$8.0^{+4.0}_{-3.2}$
Rich-H	$17.4^{+5.7}_{-4.7}$

Global models give $S_{\rm LS} \approx 29$–32 TNU (~20% uncertainty), while the **local JULOC** models predict a markedly higher signal of ~ 40–41 TNU with reduced (~10%) uncertainty — reflecting the enriched HPE content of the South China crust.

Geoneutrino Measurement in JUNO

Best fit: 72.6 ± 10.9 TNU (~15% precision)

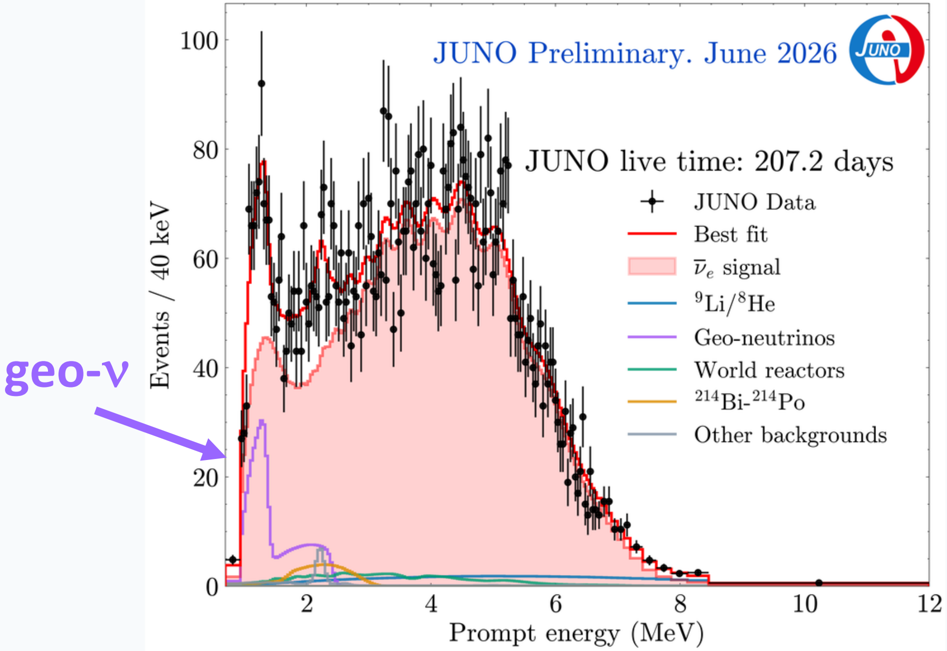

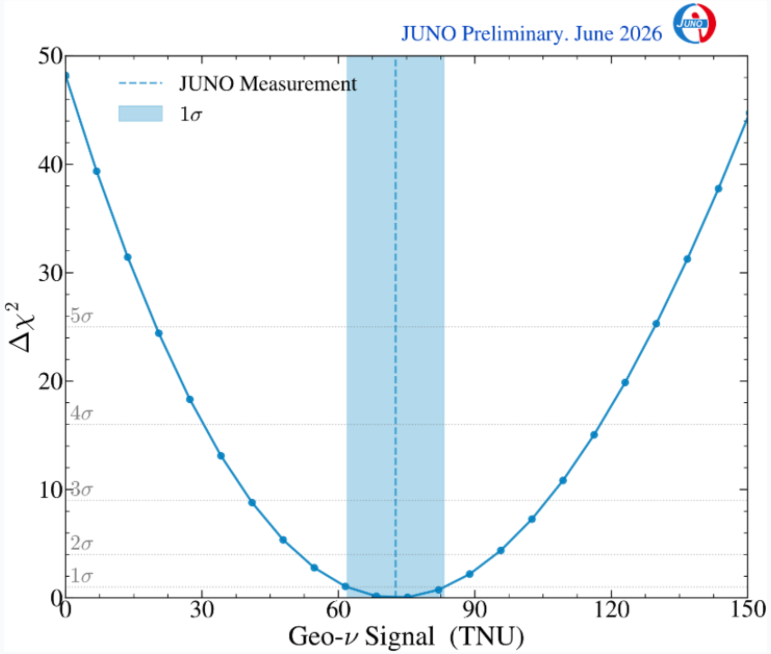

- Fit **without** geo flux constraint
- Th/U signal ratio fixed to chondritic **0.29 (±10%)**
- Zero signal excluded at $> 5\sigma$ ($\Delta\chi^2 > 48$)
- 440 ± 66 geo events from **207.2 days**

Comparing Measurements with Models

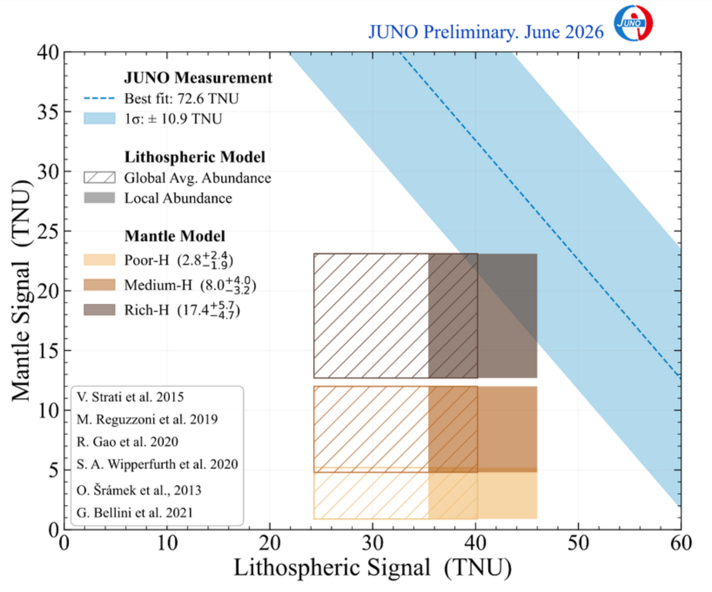

JUNO measurement vs BSE + lithospheric model combinations

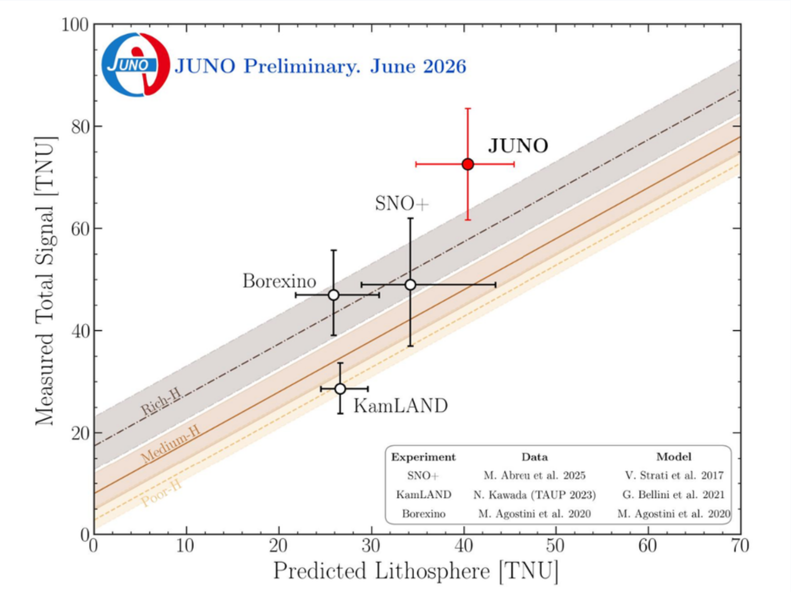

Geoneutrino signals at KamLAND, Borexino, SNO+, JUNO

- JUNO result is **higher than expectation** from existing models, but *not statistically significant*
- Hints at an **enriched U & Th content in the South China crust** — above the global average abundance
- Need more JUNO data and more refined geological model predictions

Discussion

Interpreting the JUNO measurement

The JUNO measurement ($S_{\text{tot}} = 72.6 \pm 10.9$ TNU) is **higher than most model predictions** (~ 32–59 TNU range) .

Possible explanations

- **Local crust model** — JULOC may underestimate the HPE content of the South China crust
- **CLM Th/U ratio** — Continental Lithospheric Mantle beneath South China may be enriched relative to the chondritic value adopted in current models
- **Mantle heterogeneity** — JUNO site may not represent the global average
- **Data fluctuation or unknown backgrounds?**

- Hints at **enriched U & Th content in the South China crust** — above the global average abundance
- More JUNO data needed to reduce statistical uncertainty
- Refined geological models (especially local crust) are essential

Summary

Geoneutrino Measurement

$S_{\text{tot}}(\text{U+Th}) = 72.6 \pm 10.9$ **TNU**

from **207.2 days** of JUNO data

440 ± 66 geoneutrino candidates

$> 5\sigma$ detection significance

More data needed to constrain geo-models

JUNO opens a new era of precision geoneutrino physics.

Radiogenic Heat and Mantle Signals

From geoneutrino signal to mantle radiogenic heat

- The expected mantle geoneutrino signal S_M for each BSE class follows a **linear relation** between mantle heat H_M and signal: $S_M = \beta \cdot H_M$, where β depends only on the U/Th spatial distribution in the mantle.
- $S_M = S_{\text{tot}} - S_{\text{LS}}$, and $H_{\text{total}} = H_{\text{LS}} + H_M/[\beta\,(1 - f_K)]$, where $f_K = 0.17$ accounts for the undetectable ^{40}K heat.
- β ranges from **0.75** (HPEs at the core–mantle boundary) to **0.98** (homogeneous mantle), with central value $\beta = 0.86$[1].

> The global surface heat flow is $Q_{\text{surf}} = 47 \pm 2$ **TW**[2]

[1] JUNO Collaboration (T. Adam et al.), "Prospects for geoneutrino detection with JUNO", arXiv:2511.07227 [hep-ex] (2025)

[2] J. H. Davies and D. R. Davies, *Earth's surface heat flux*, Solid Earth 1, 5–24 (2010)

Litho Model	S_{LS} (TNU)	S_M (TNU)	$\beta = 0.75$ (TW)	$\beta = 0.86$ (TW)	$\beta = 0.98$ (TW)
RRM	$30.9^{+6.5}_{-5.2}$	$41.7^{+12.1}_{-12.7}$	$75.1^{+19.5}_{-20.4}$	$66.5^{+17.0}_{-17.8}$	$59.4^{+15.0}_{-15.7}$
GIGJ	$28.9^{+5.5}_{-4.4}$	$43.7^{+11.8}_{-12.2}$	$78.3^{+19.0}_{-19.7}$	$69.3^{+16.6}_{-17.2}$	$61.8^{+14.6}_{-15.1}$
W20 [Crust2.0]	$32.0^{+8.2}_{-6.6}$	$40.6^{+12.7}_{-13.6}$	$73.3^{+20.6}_{-22.0}$	$65.0^{+18.0}_{-19.2}$	$58.0^{+15.8}_{-16.8}$
W20 [Crust1.0]	$31.7^{+8.4}_{-6.6}$	$40.9^{+12.7}_{-13.8}$	$73.8^{+20.6}_{-22.2}$	$65.4^{+18.0}_{-19.3}$	$58.4^{+15.8}_{-17.0}$
W20 [Litho1.0]	$30.7^{+8.1}_{-6.4}$	$41.9^{+12.6}_{-13.6}$	$75.4^{+20.4}_{-21.9}$	$66.8^{+17.8}_{-19.1}$	$59.6^{+15.7}_{-16.8}$
JULOC	$40.4^{+5.6}_{-5.0}$	$32.2^{+12.0}_{-12.3}$	$59.8^{+19.4}_{-19.7}$	$53.2^{+16.9}_{-17.2}$	$47.7^{+14.9}_{-15.1}$
JULOC-I	$41.2^{+4.6}_{-3.3}$	$31.4^{+11.4}_{-11.8}$	$58.5^{+18.4}_{-19.1}$	$52.1^{+16.1}_{-16.6}$	$46.7^{+14.1}_{-14.6}$

Combination of Different Experiments

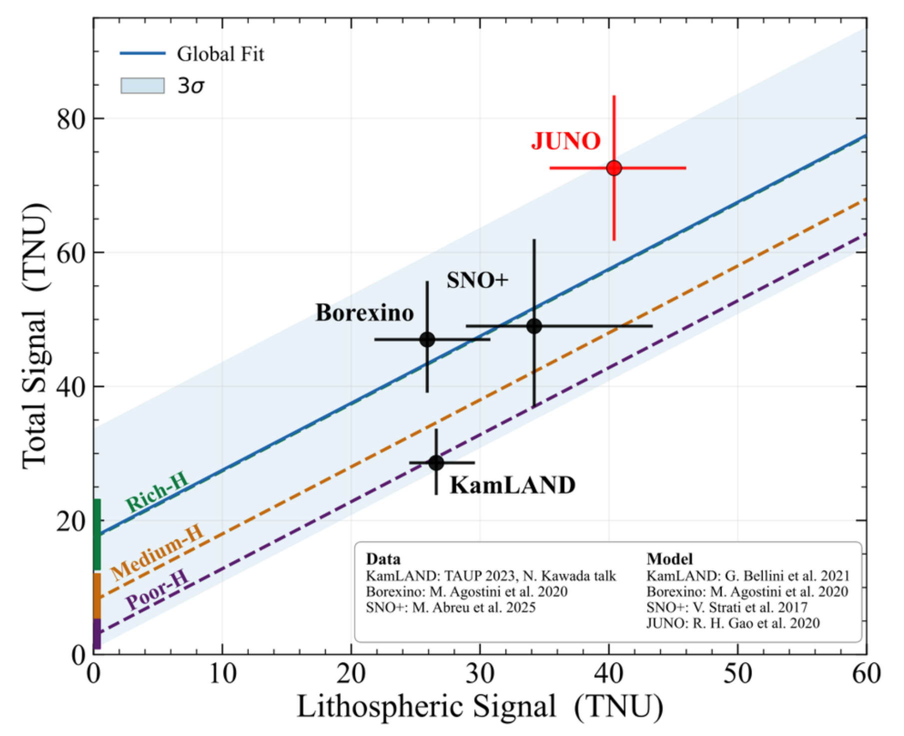

$$17.5^{+5.4}_{-5.6}$$

Best-fit intercept S_{M} (TNU)

- Four experiments: **JUNO + KamLAND + Borexino + SNO+**
- S_{tot} vs predicted S_{LS} at each site
- Unit-slope fit: $S_{\mathrm{tot}} = S_{\mathrm{LS}} + S_{\mathrm{M}}$
- Intercept = **common mantle signal**